

MODIS DATA STUDY TEAM PRESENTATION

October 21, 1989

AGENDA

1. The Landsat Worldwide Reference Systems
2. Retrieval of Chlorophyll Fluorescence and Its Impact on Atmospheric Corrections, Part 2
3. Coccolithophore Reflectance and Cells/Milliliter Measurement Relationships
4. Preliminary Estimates of MODIS Core Data Product Accuracies and Their Relevance to Key Earth Science Issues

THE LANDSAT WORLDWIDE REFERENCE SYSTEMS

The Earth Resources Browse Facility (ERBF) exists to provide users of Landsat Thematic Mapper (TM) and Multispectral Scanner (MSS) data with a browse data source. The primary contacts are Locke Stuart (Earth Resources Data Applications Manager; 286-5411) or Susan Mentzey (286-5170). The ERBF capabilities were investigated and assessed against the MODIS science requirements for data acquisition; specifically, metadata, browse data, and MODIS data product ordering and delivery.

1. Description of the Landsat Worldwide Reference Systems (WRS)

Due to the different orbital altitude and periods, a different WRS exists for Landsat 1,2, and 3 versus that of Landsat 4. The former WRS consists of a global network of 251 paths (standard orbits). The Landsat-4 was launched into a 705 km sun-synchronous orbit (versus 919 km for the previous spacecraft), which yields 233 consecutive orbits for a 16-day repeat period. The coordinate system used to identify and catalog Landsat-4 scenes is based on the 233 paths and 119 rows. The rows are numbered southward, beginning at 80°N, while the orbit paths are numbered westward with path number 001 passing through eastern Greenland and South America.

The WRS is indexed around 26 "sheets", 13 for each hemisphere. The sheets cover 100% of the planet. For example, Sheet 11 covers northern Africa and the Mediterranean Sea, and extends from the equator to 40°N and from about 20°W to 50°E (Figure 1).

Once the user has accessed the appropriate sheet and identified the desired path/row coordinates, the catalog listing of all available scenes for that region may be accessed interactively. For example, for path 196, row 45, a total of 12 MSS scenes were identified.

For each scene, a limited amount of metadata exists, including the latitudes and longitudes of the four corners, the percentage of cloud cover, a measure of the quality of the data, and the form and medium of the available data. By selecting cloud cover <10%, nine scenes were identified. By selecting 0% cloud cover and the highest quality, four MSS scenes remained. The available information for these scenes is illustrated in Figure 2. The data may then be browsed using whatever hard-copy media are available in the ERBF, or ordered.

2. Analysis of Strengths Relative to the MODIS Science Requirements

As an analog to data browse facilities to be made available under EosDIS, the capabilities of the ERBF meet some important requirements.

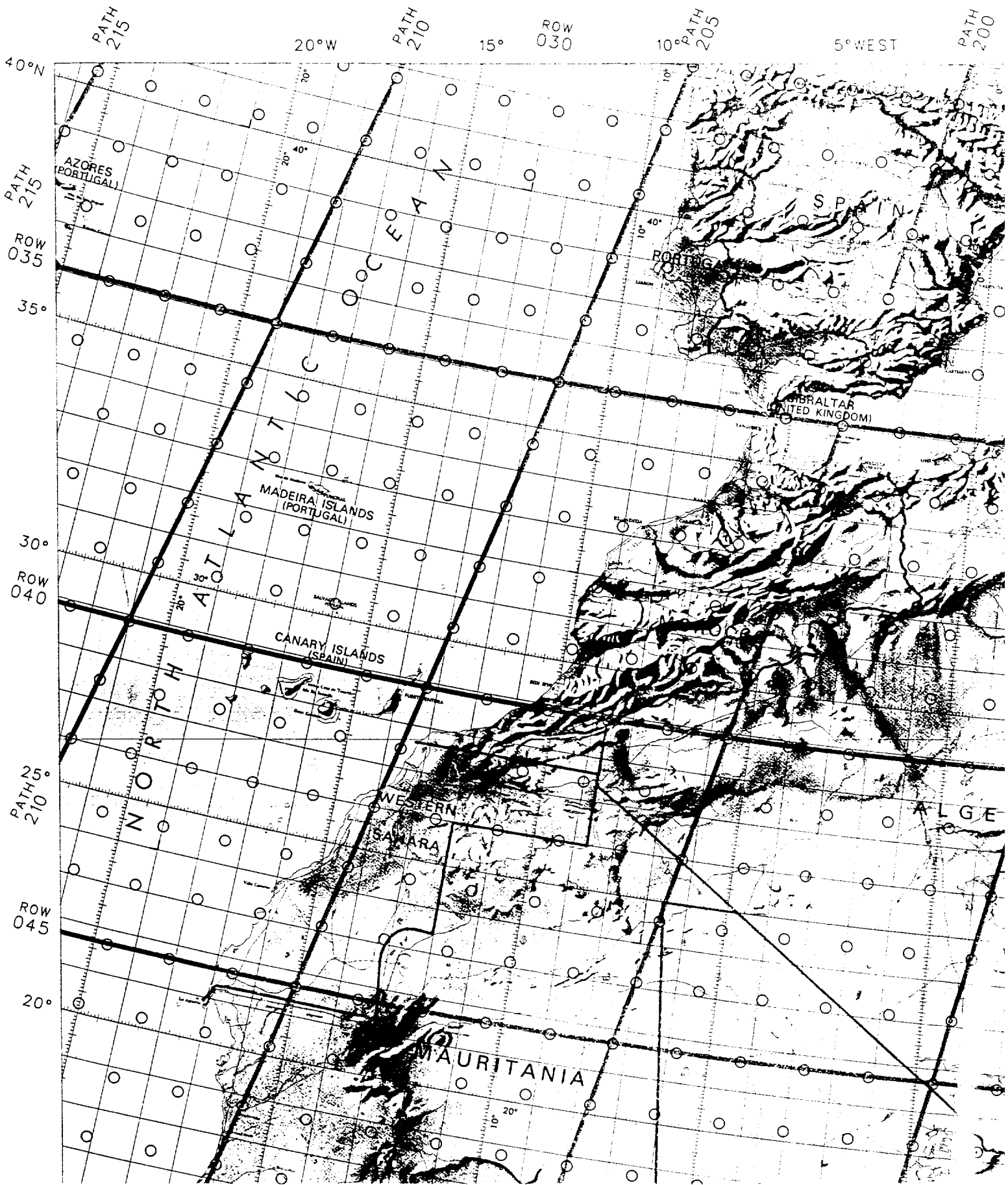
- A standard reference coordinate system is available to relate multiple views of any region. In fact, due to the anticipated 705 km orbit of the polar platform, a similar or identical coordinate system could be used for MODIS (though the spatial coverage for a scene would be considerably larger).
- With little information, the user can identify all data available for a region of interest.
- The system can be learned and used productively in minutes, with no advance knowledge on the part of the user required.
- Some information is available to assist the user in selecting those data that most meet the user's requirements (e.g., precise position of the scenes, cloud coverage over the scene, and quality information).

3. Analysis of Weaknesses Relative to the MODIS Science Requirements

- To use the system, a set of 26 charts, an interactive data base, and microfiche must be accessed to locate, identify, screen, and browse a given scene. For MODIS data, this set

of procedures should all be performed interactively during the same session. For MODIS, the Level-1B radiance data (and atmospherically corrected Level-2 radiances) for a subset of the bands, along with selected Level-2 and Level-3 standard data products, will be available as browse data.

- MODIS, unlike Landsat TM and MSS, will observe the Earth on a full-time basis, observing any region of the surface on practically a daily basis. During the course of a five to 15 year mission, many hundreds of scenes will be obtained for any given path and row. Furthermore, due to the overlap between adjacent paths and rows, many thousands of MODIS scenes will be available for the user to select. Often, the user may be interested in developing time series or studying trends over a region, and may select many overlapping scenes over a given time-frame. Therefore, a more flexible cataloging and ordering system will be required.
- The data access system for MODIS must support a much greater variety of derived data products than that for Landsat TM and MSS. Derived data products will need to be displayed to support selective access, and each product may require unique metadata elements appropriate only to that product or closely related products. The larger volumes of data and number of products to be accessed will force the development of very efficient, fully automated data selection techniques that are not required to access data in smaller, less complex data systems.



ENTER DEPIPED RETRIEVAL DATA.

PN 196,51 SA:45

12 ACCESSIONS.

PN 196,51 SA:45 CL:1

9 ACCESSIONS.

PN 196,51 SA:45 CL:0 DU:8

4 ACCESSIONS.

DEI

IX (ACCESSION INDEX) FOR PRIMARY ACCESSIONS.
LS (LANDSAT) 4

1 85098309505X0 86 ***** 8888*** 00 B&W-06.7" N13D01M008 W003D09M008
2 LANDSAT-E (MSS) 11/09/84 1000000 196 51 LCPEY** D7902990673
3 3806 FILM CHIP *** 137 ** 170X185 **,**,**,**
4 N133631 W0020900 N135217 W0034734 N122529 W0040842 N120943 W0023043
5 ***** 8888*** ***** NYNND8+S FILM CHIP ADB007704000000000 *
5 ***** ***** ***** ***** *****+LSS HDTA MASTER BKLEMHAB6315010000 *

1 85095109520X0 92 ***** 8888*** 00 B&W-06.7" N13D01M008 W003D07M008
2 LANDSAT-E (MSS) 10/08/84 1000000 196 51 LC7EY** D7902961159
3 3806 FILM CHIP *** 137 ** 170X185 **,**,**,**
4 N133631 W0020700 N135217 W0034534 N122529 W0040842 N120943 W0022843
5 ***** 8888*** ***** NYNND8+S FILM CHIP ADB007823000000000 *
5 ***** ***** 7***** BG R NYNND8+S STANDARD CCP AR85095109520X0000 *
5 ***** ***** ***** ***** *****+LSS HDTA MASTER BKLEMHAB6283310000 *

1 85074309582X0 1 ***** 8888*** 00 B&W-06.7" N13D01M008 W003D06M008
2 LANDSAT-E (MSS) 03/14/85 1000000 196 51 LC7EY** D7902720976
3 3806 FILM CHIP *** 137 ** 170X185 **,**,**,**
4 N133631 W0020600 N135217 W0034434 N122529 W0040542 N120943 W0022743
5 ***** 8888*** ***** NYNND8+S FILM CHIP ADB007183000000000 *
5 ***** ***** 7***** BG R NYNND8+S STANDARD CCP AR85074309582X0000 *
5 ***** ***** ***** ***** *****+LSS HDTA MASTER BKLEMHAB6074030000 *

1 85026310020X0 105 ***** 8888*** 00 B&W-06.7" N13D00M008 W003D00M008
2 LANDSAT-E (MSS) 11/19/84 1000000 196 51 LC7EY** D7902350966
3 3806 FILM CHIP *** 137 ** 170X185 **,**,**,**
4 N133531 W0020001 N135117 W0033834 N122429 W0035942 N120843 W0022143
5 ***** 8888*** ***** NYNND8+S FILM CHIP ADB007061000000000 *
5 ***** ***** 7***** BG R NYNND8+S STANDARD CCP AR85026310020X0001 *
5 ***** ***** ***** ***** *****+LSS HDTA MASTER BKLEMHAB4325060000 *

DONE

ENTER NEW TRANSACTION

Retrieval of Chlorophyll Fluorescence
and Its Impact on Atmospheric Corrections
Part 2

Chlorophyll fluorescence occurs at wavelengths where the water-leaving radiance is assumed zero for Case 1 oceanic atmospheric correction algorithms. These Case 1 algorithms apply for most of the world's oceans (about 90%) and will probably be assumed for routine ocean processing. However, chlorophyll fluorescence conflicts with the assumptions of the Case 1 atmospheric correction algorithms by producing water-leaving radiance at the MODIS-T bands at 665, 680, 695, and 710 nm. We wondered if fluorescence was retrievable under routine processing and whether a flag could be developed to alert the processing procedure to such fluorescence, and secondly, what errors are involved in the case of fluorescence for the computation of chlorophyll. Any specific algorithm to correct for these effects will, of course, have to be developed by the MODIS Science Team, but we wanted to examine an area of potential concern for the MODIS processing scenario.

Plots of the normalized water-leaving radiance (the radiance assuming a solar zenith at nadir and with the atmosphere removed) have been generated for different chlorophyll concentrations. The model of Sathyendranath and Platt (1988) was used to obtain the optical properties and the model of Gordon et al. (1988) was used to convert these optical properties into water-leaving radiances $[L_w]_N$ (Figure 1). We assumed that only chlorophyll and water affected the optical properties of the water, and plotted results for 0.05, 0.5, 1.0, 5.0, and 10.0 mg chl m^{-3} , weighted as the mean signal over the MODIS-T bands. The addition of chlorophyll fluorescence as an increase in reflectance of 0.02% per mg m^{-3} chlorophyll (Gower and Borstad, 1983) produced a change in $[L_w]_N$ near 685 nm as shown in Figure 2. Again the reflectance change was weighted over the MODIS-T wavelengths.

These normalized water-leaving radiances were used to generate a simulated radiance signal received by MODIS-T by assuming a single scattering approximation for Rayleigh scattering (with Rayleigh optical thickness computed from Gordon et al., 1988), an ozone scale height of 0.333 cm, and an aerosol radiance of 0.19 mW $cm^{-2} \mu m^{-1} sr^{-1}$ at 865 nm with an Angstrom exponent of -0.3, i.e., typical of maritime atmospheres (Gregg and Carder, 1989). The normalized water-leaving radiances were converted to simulated water-leaving radiances L_w assuming a solar zenith angle of 30° and an atmosphere as described. From these simulated Rayleigh, aerosol, and water-leaving radiances, we computed the total simulated radiance observed by MODIS-T L_t by summing. The simulated water-leaving radiances produced chlorophyll concentrations of 0.025, 0.111, 0.239, 3.65, and 4.94 mg m^{-3} using the CZCS bio-optical algorithms, relating the water-leaving

radiance at 443 nm (or 520 nm for concentrations > 1.5) to 550 nm. The difference between these concentrations and the original concentrations used to generate the normalized water-leaving radiances is due to the fact that no optically active substances other than chlorophyll were included in the original model, and the CZCS algorithm is empirical. These values are used for determination of errors in the succeeding sections.

We then applied the proposed (Gordon, 1989) atmospheric correction algorithm for Case 1 waters to these simulated total radiances L_t . In this correction we again assumed single scattering for the Rayleigh correction. The proposed Case 1 algorithm assumes no water-leaving radiance at 875, 755, and 665 nm. Angstrom exponents are calculated at these wavelengths and the mean of the Angstrom exponents at 755 and 665 nm is used to extrapolate to smaller wavelengths.

These Angstrom exponents are shown in Figure 3. They remain stable for low chlorophyll, but at high chlorophyll (> 1 mg m⁻³) deviate from the general pattern between 665 and 710 nm. This is because the Sathyendranath and Platt model predicts large backscattering from high chlorophyll concentrations in this spectral region. These exponents produce some scatter in the aerosol radiances at lower wavelengths (Figure 4). However, chlorophyll concentrations predicted from the resulting water-leaving radiances (Figure 5) ranged from 6 to 37% error as determined from the original chlorophyll values.

Atmospheric correction after the addition of chlorophyll fluorescence to the water-leaving radiance yielded Angstrom exponents that deviated greatly from the mean near 680 nm, now nearly twice as low as the computations without fluorescence for high chlorophyll (Figure 6). Furthermore, because of the assumption that the water-leaving radiance is zero for $k > 665$ nm, there is no evidence of fluorescence in the retrieved water-leaving radiances (Figure 7). The fluorescence is apparent, however, in the aerosol radiances (Figure 8). These results suggest two possibilities for the MODIS routine processing scenario: 1) that Angstrom exponents can be used as a flag to determine the existence of fluorescence, and 2) the fluorescence is retrievable in the routine Case 1 processing scenario through the aerosol radiances rather than the water-leaving radiances. The error in subsequent chlorophyll algorithms in the presence of fluorescence is not large; within 7 to 30% except at the highest concentration, where the error was 77%.

Next we applied the proposed Case 2 algorithm to investigate the effects of fluorescence on chlorophyll concentrations and its retrievability under these conditions. This algorithm requires only that the water-leaving radiance at 875 and 755 nm be zero. The Case 2 algorithm produced a set of Angstrom exponents that were very smooth across the spectrum (Figure 9), and very near the -0.3

value from which the original aerosols were generated. These Angstrom exponents produced aerosol radiances that were constant with chlorophyll concentration (Figure 10), as they were originally. Furthermore, the fluorescence signal was not evident in these aerosol radiances. Instead, the fluorescence signal appeared in the water-leaving radiances (Figure 11), where they originate in reality, suggesting the feasibility of the Case 2 algorithm in detecting fluorescence. The Case 2 algorithm also reduced the errors in chlorophyll retrievals especially at high concentrations, now ranging from 1 to 3%.

These simulations suggest that the fluorescence signal is in fact retrievable from the MODIS routine processing scenario, regardless of whether the Case 1 or Case 2 algorithms are used. The only difference is where the signal will appear: in the Case 1 algorithm fluorescence appeared in the aerosol radiances while in the Case 2 algorithm it appeared in the water-leaving radiances. The method for routinely determining fluorescence has not yet been defined, but it is encouraging that the signal appears in pre-launch core data products (aerosol and water-leaving radiances) regardless of the method of atmospheric correction for aerosols (Case 1 or Case 2). Furthermore, these simulations suggest the possibility of using the Angstrom exponents, another pre-launch core data product, as a flag to detect the presence of fluorescence. At high concentrations and high fluorescence, the computed Angstrom exponent was substantially lower at 665 nm than at 755 nm. Thus, a possibility for routine MODIS data processing might be to assume Case 1 waters and observe the behavior of the Angstrom exponent at 665 nm to yield a clue to the presence of fluorescence. Scenarios for MODIS data processing may change as the method for flagging and detecting fluorescence change, but a preliminary scenario may be formulated with knowledge that the fluorescence signal will not be lost.

References

- Gordon, H.R., 1989. Algorithm development for ocean observation with EOS/MODIS. MODIS Science Team Member Report.
- Gordon, H.R., D.K. Clark, J.W. Brown, O.B. Brown, R.H. Evans, and W.W. Broenkow, 1983. Phytoplankton pigment concentrations in the Middle Atlantic Bight: comparison of ship determinations and CZCS estimates. *Applied Optics* 22: 20-36.
- Gordon, H.R., O.B. Brown, R.H. Evans, J.W. Brown, R.C. Smith, K.S. Baker, and D.K. Clark, 1988. A semianalytic radiance model of ocean color. *Journal of Geophysical Research* 93: 10909-10924.
- Gower, J.F.R. and G. Borstad, 1983. Use of the in-vivo

fluorescence line at 685 nm for remote sensing surveys of surface chlorophyll a. In: Oceanography from Space. pp. 329-338.

Gregg, W.W. and K.L. Carder, 1989. A simple, very high spectral resolution solar irradiance model for cloudless maritime atmospheres. Limnology and Oceanography, submitted.

Sathyendranath, S. and T. Platt, 1988. The spectral irradiance field at the surface and in the interior of the ocean: a model for applications in oceanography and remote sensing. Journal of Geophysical Research 93: 9270-9280.

Normalized Water-Leaving Radiances without Fluorescence

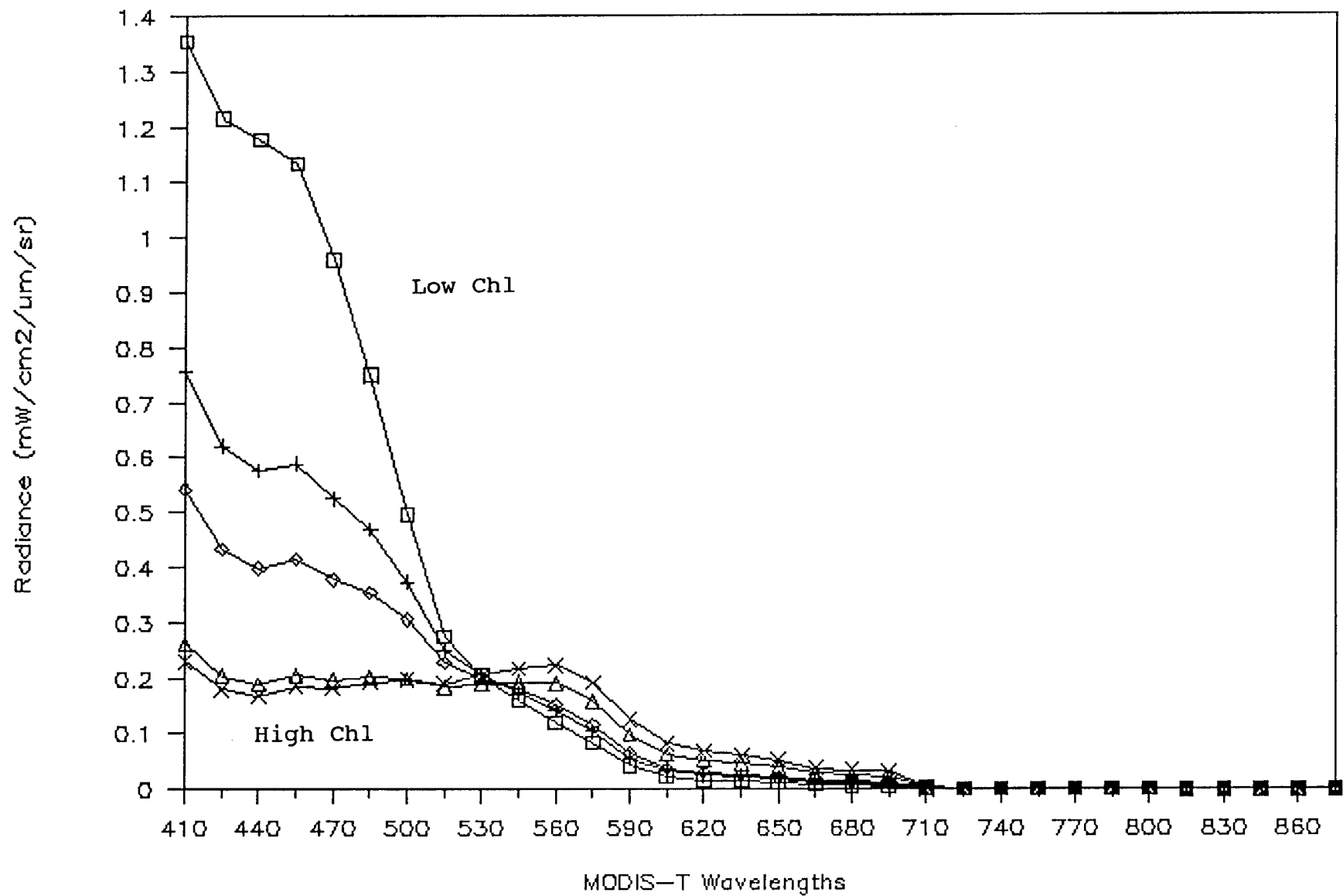


FIGURE 1.

Normalized Water-Leaving Radiances

with Fluorescence

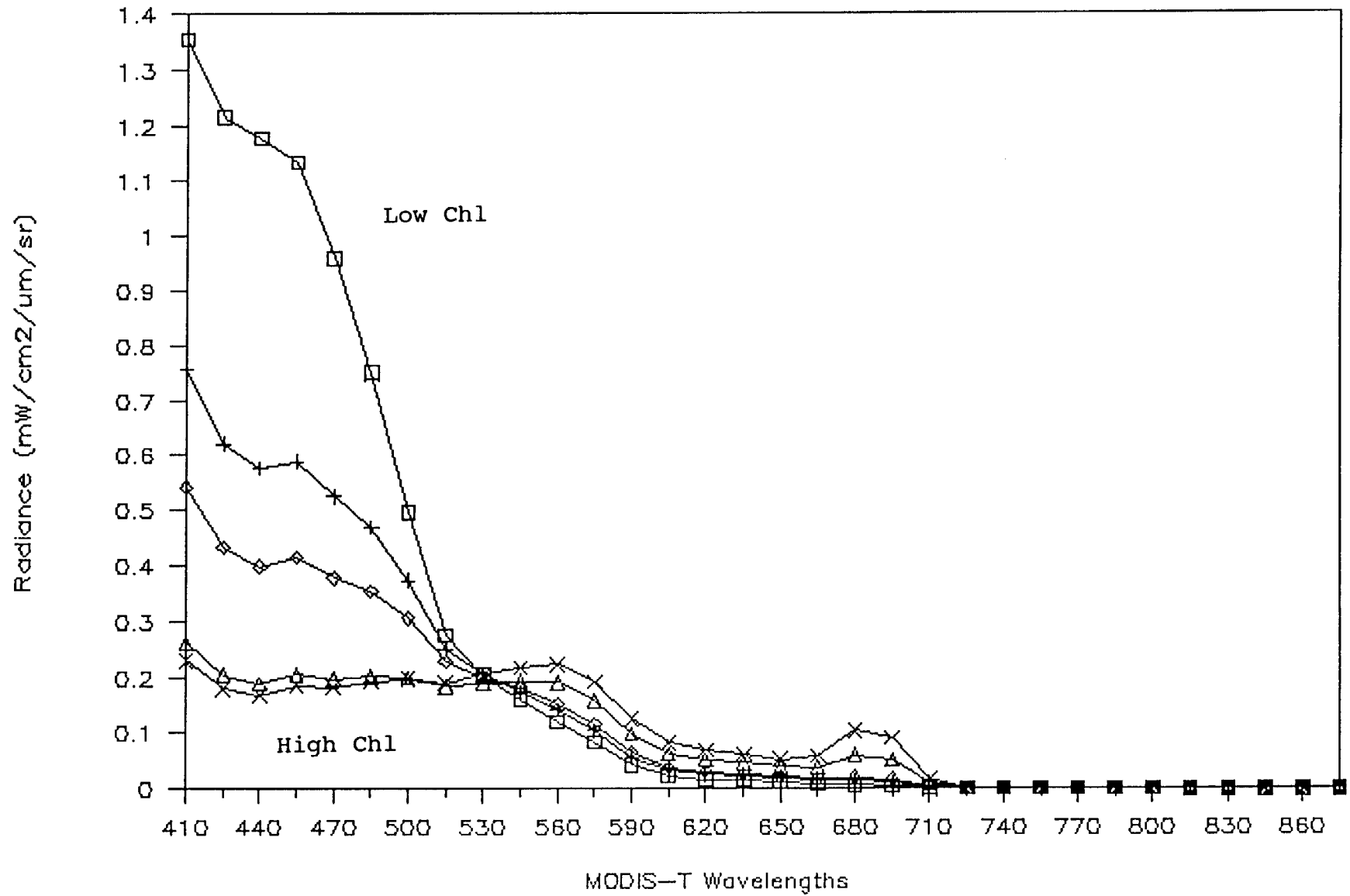


FIGURE 2.

Angstrom Exponents

without Fluorescence

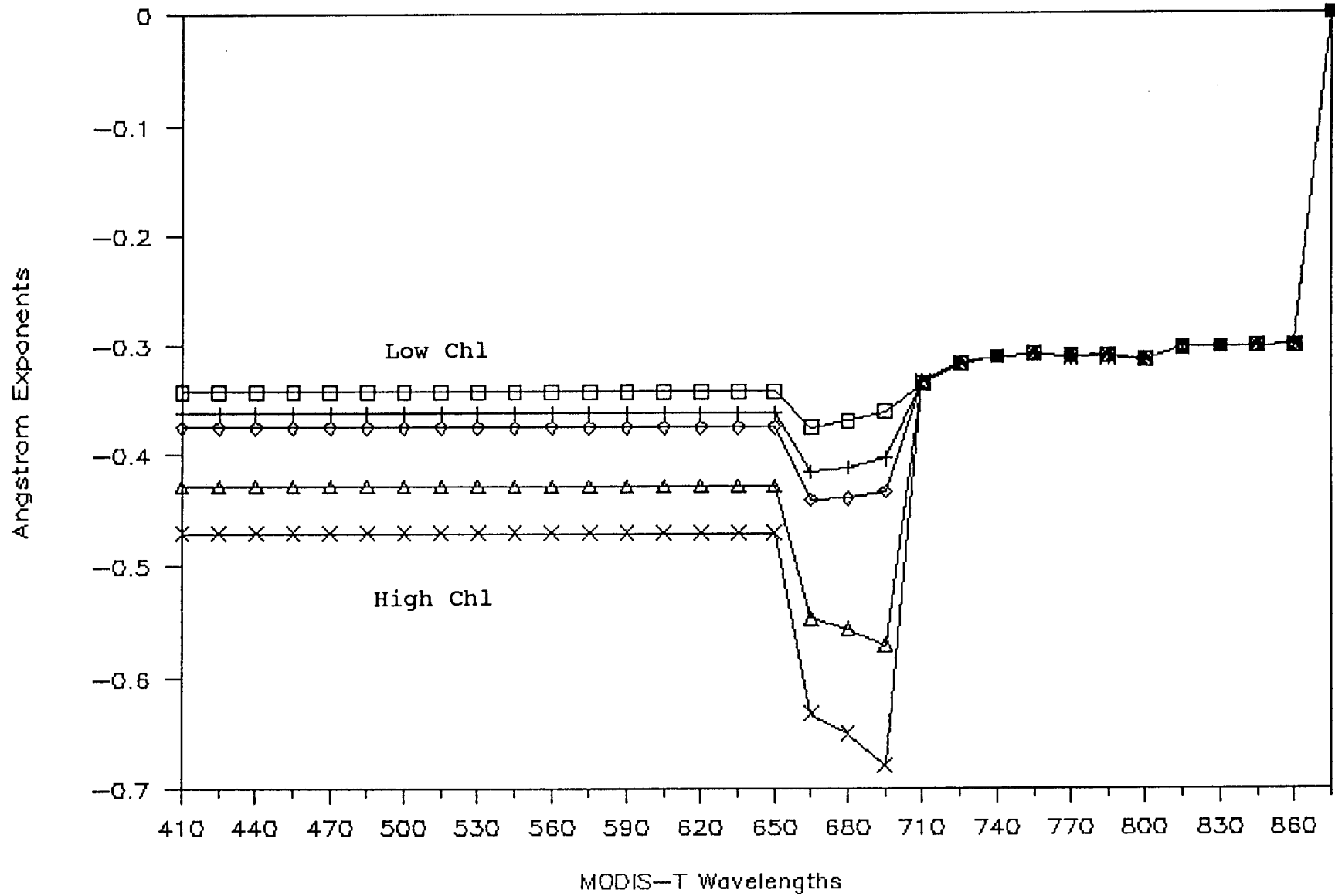


FIGURE 3.

Aerosol Radiances without Fluorescence

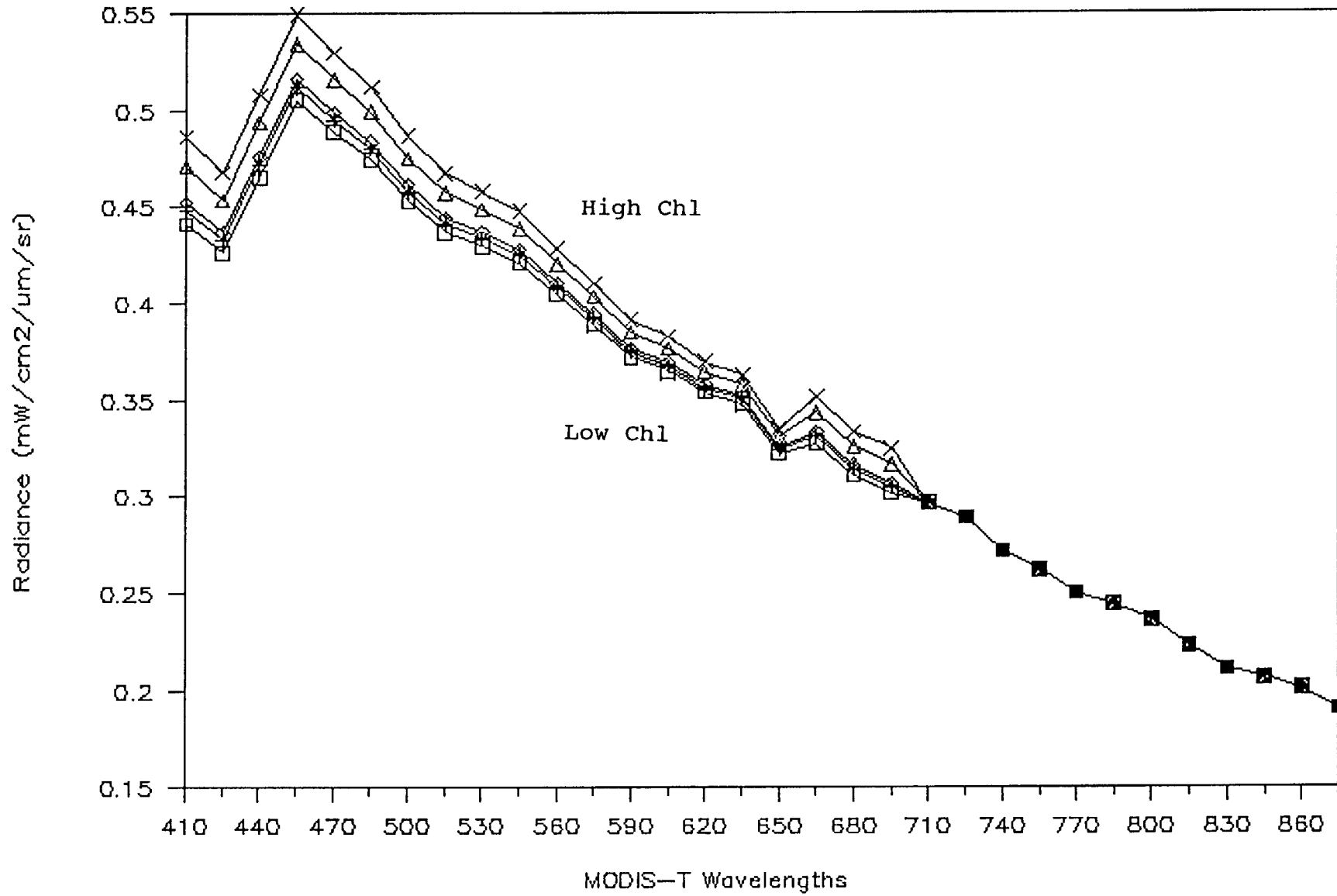


FIGURE 4.

Water-Leaving Radiances without Fluorescence

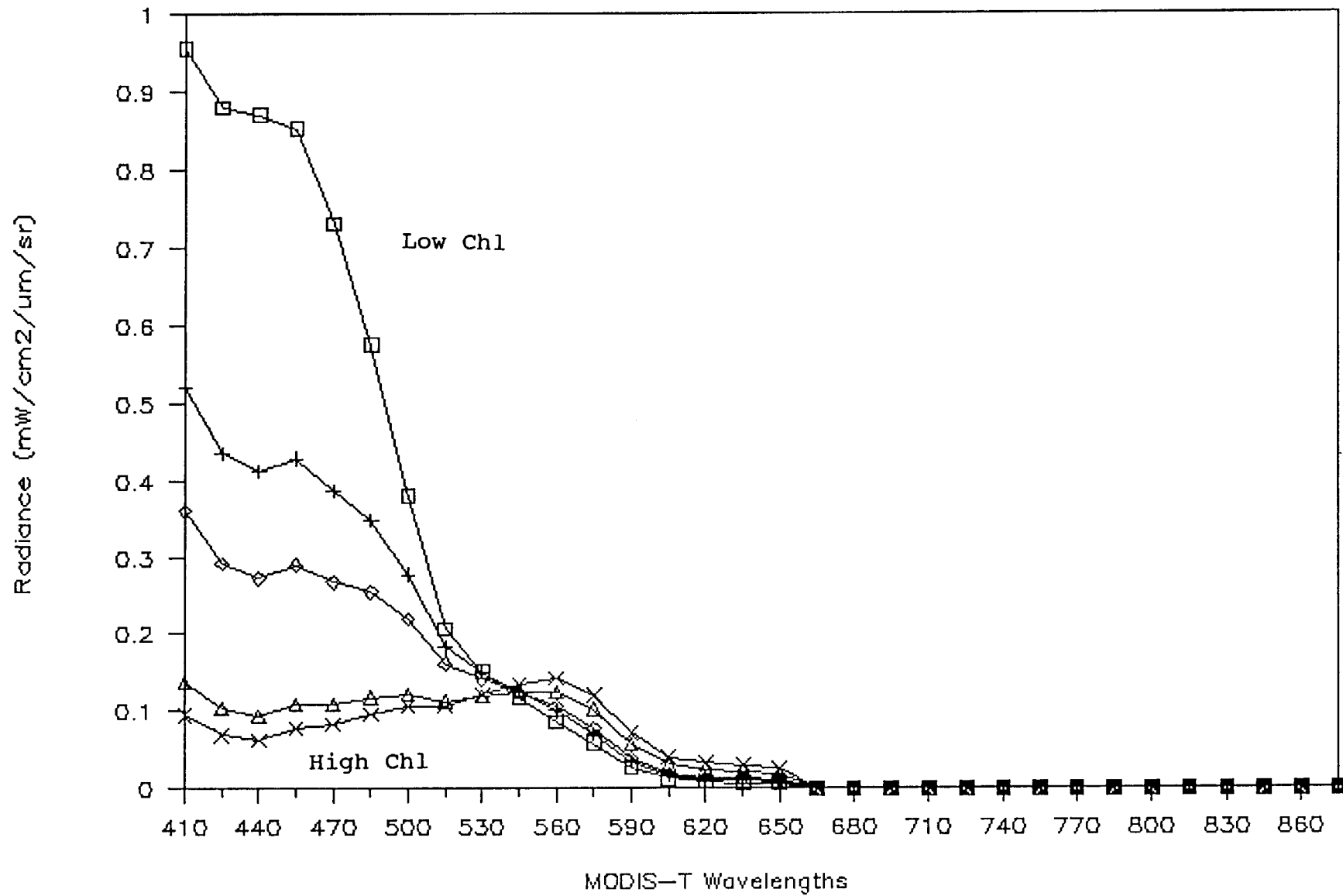


FIGURE 5.

Angstrom Exponents

with Fluorescence

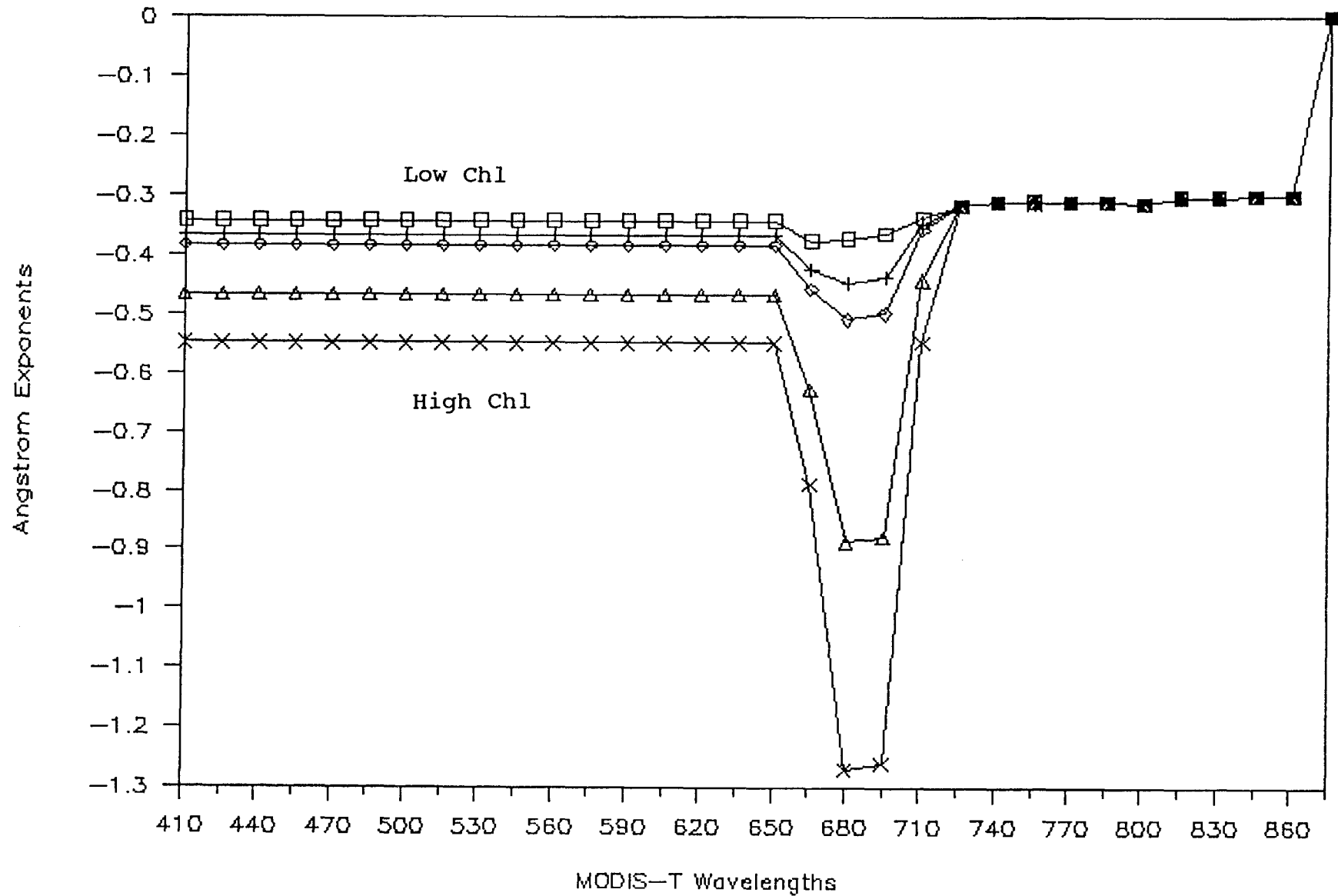


FIGURE 6.

Water-Leaving Radiances

with Fluorescence

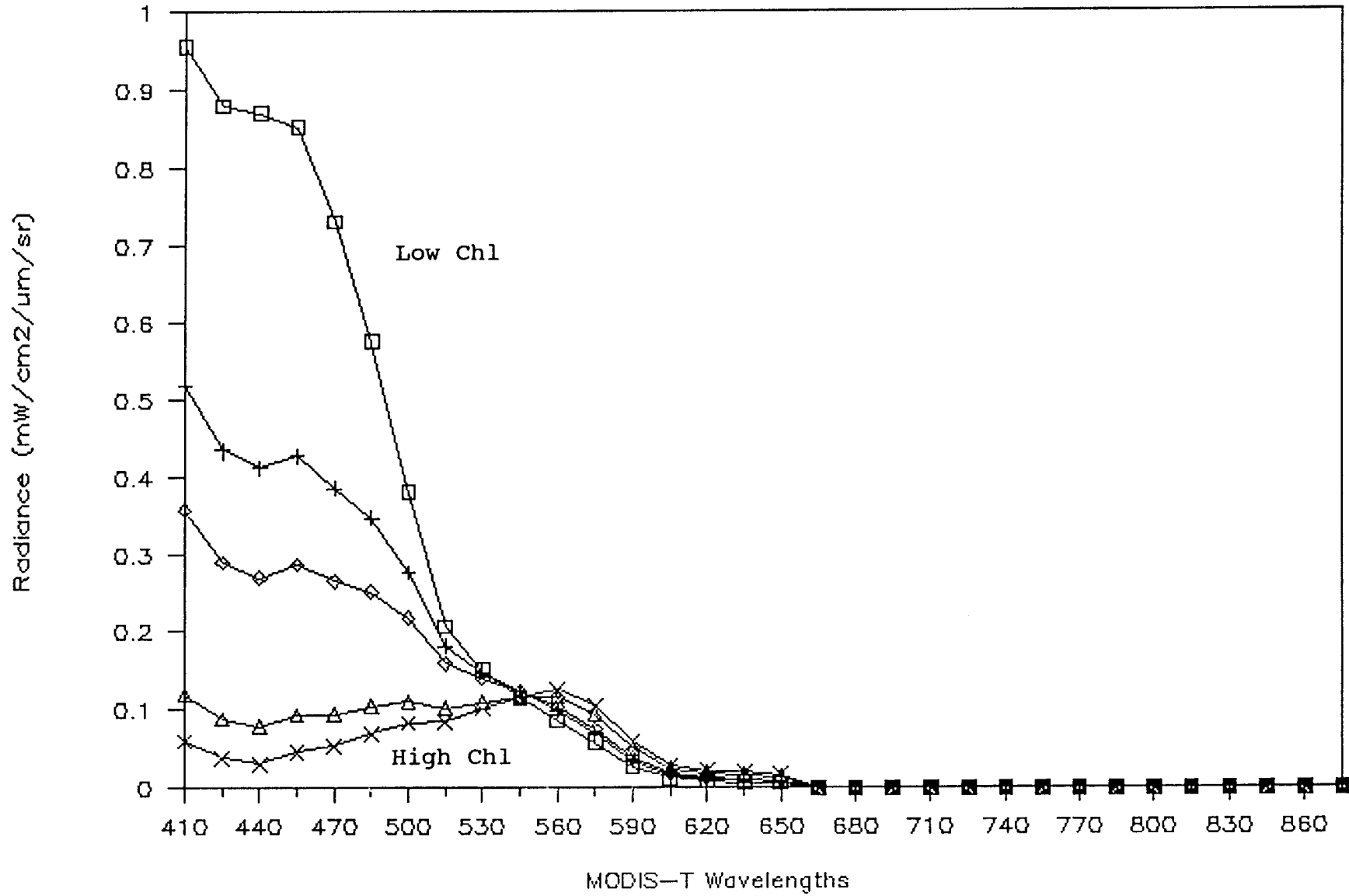


FIGURE 7.

Aerosol Radiances

with Fluorescence

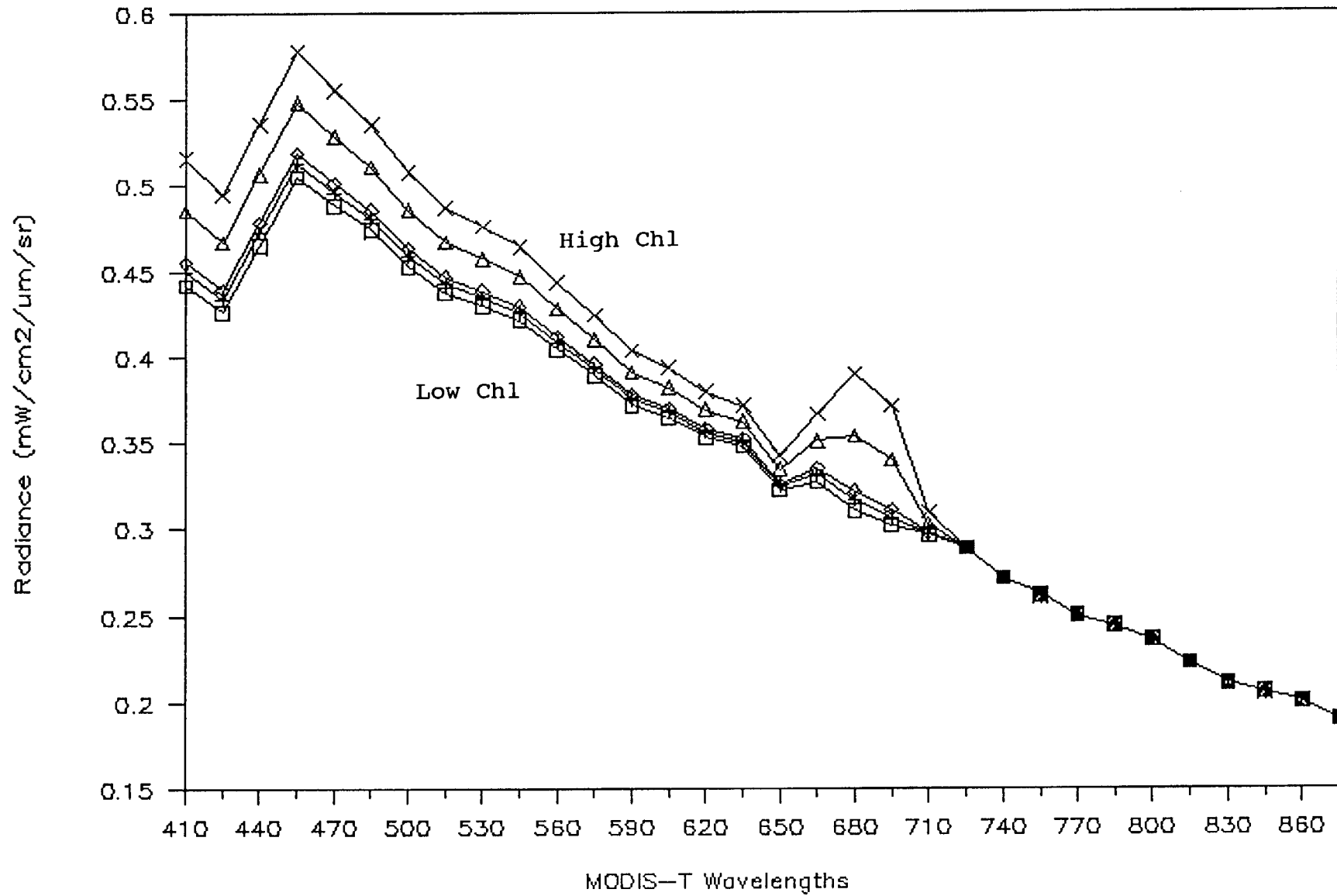


FIGURE 8.

Angstrom Exponents, Case 2

with Fluorescence

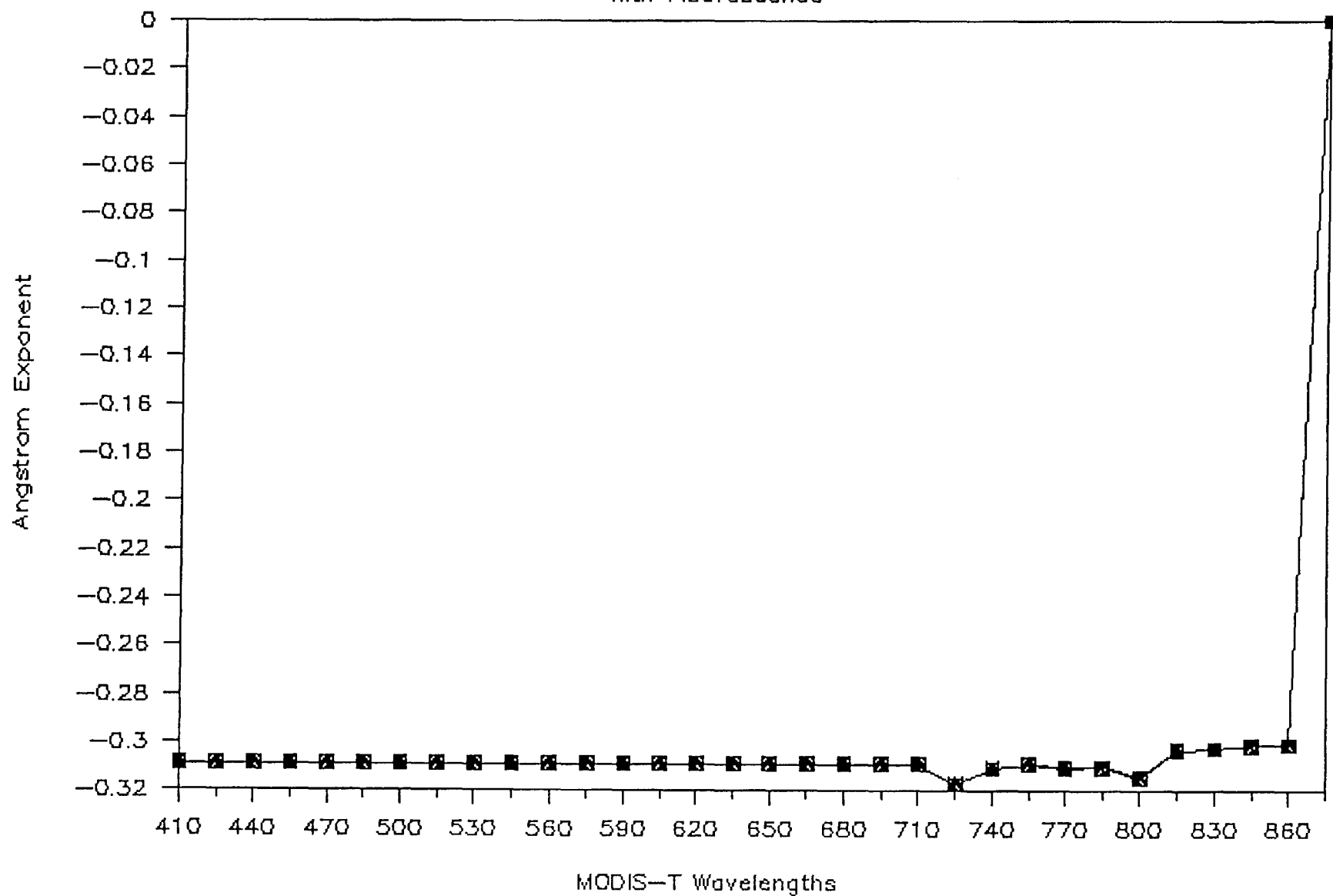


FIGURE 9.

Aerosol Radiances, Case 2

with Fluorescence

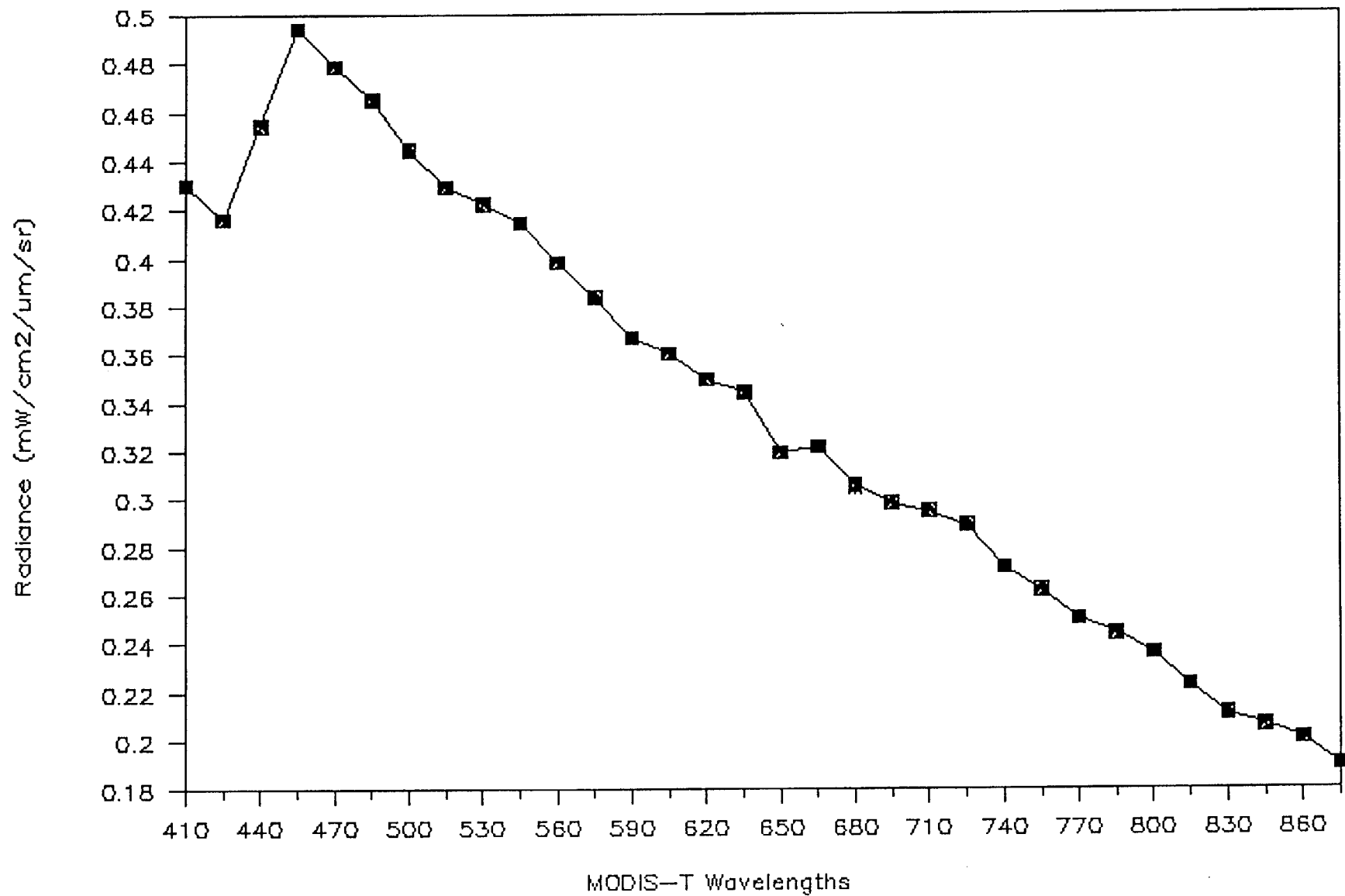


FIGURE 10.

Water-Leaving Radiances, Case 2

with Fluorescence

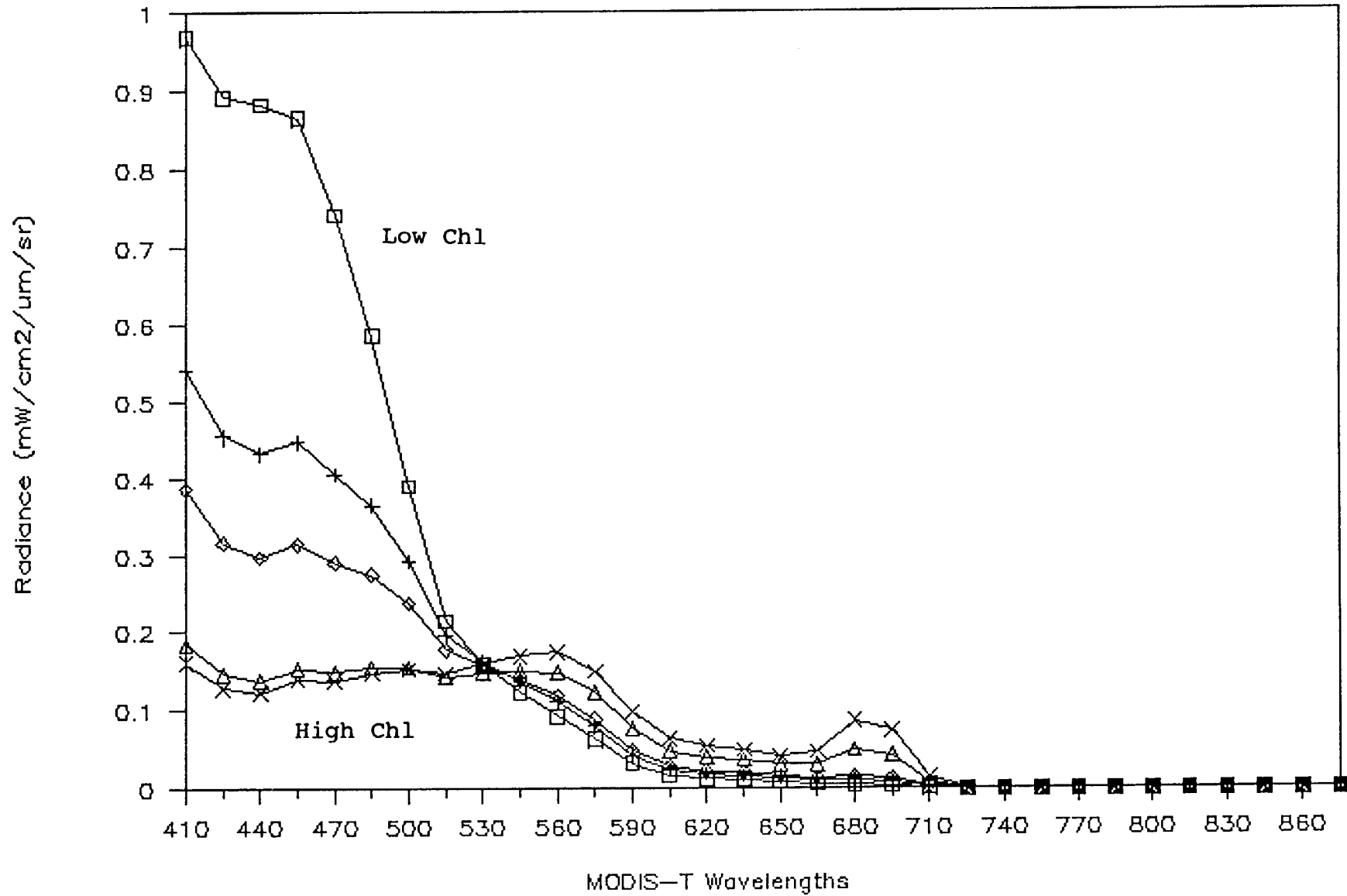


FIGURE 11.

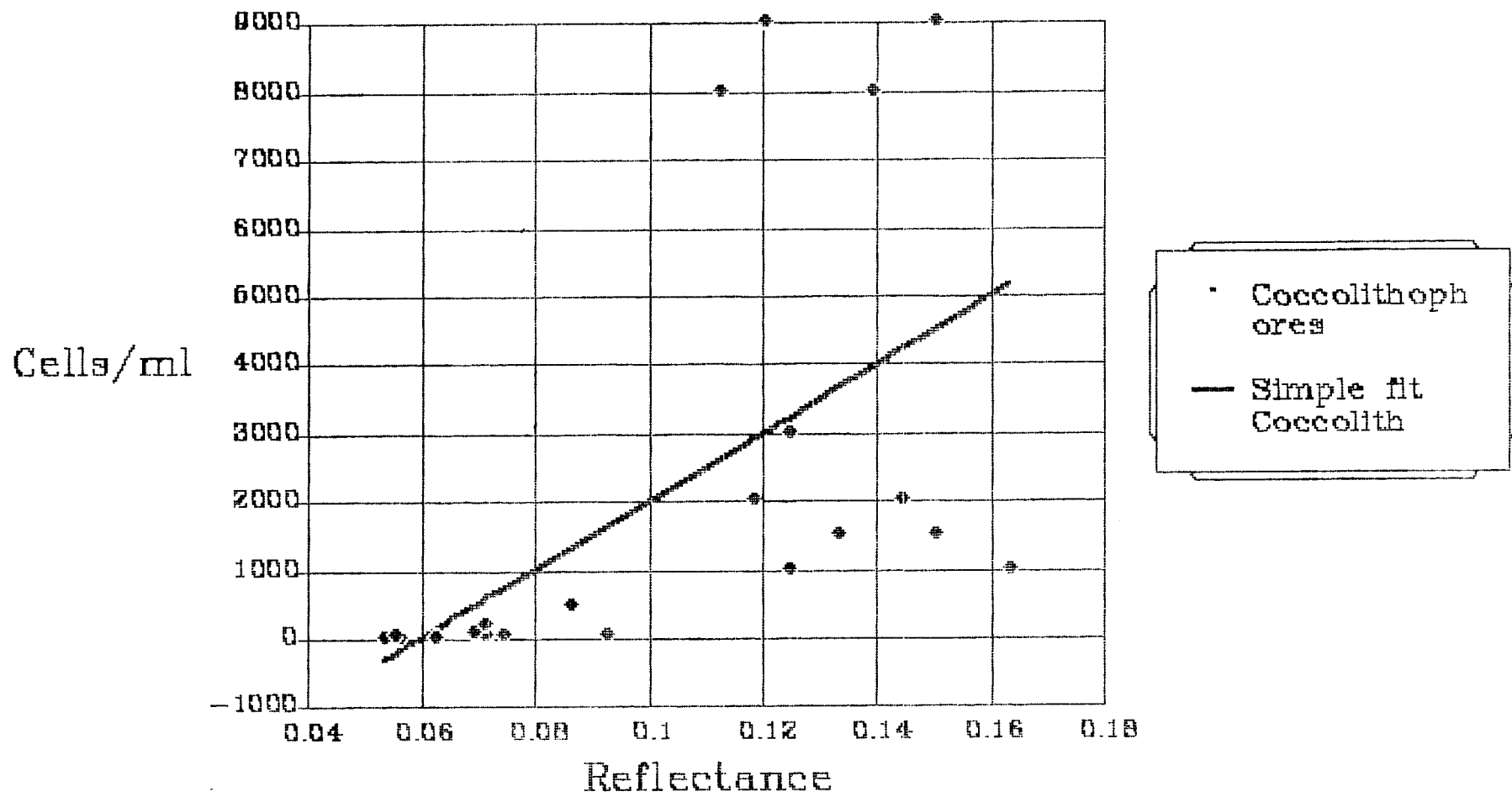
COCCOLITHOPHORE REFLECTANCE AND CELLS/MILLILITER MEASUREMENT RELATIONSHIPS

Holligan et al. (1983) presented coccolithophore measurements obtained from shipboard in situ observations. The dominant coccolithophore present in the surface bloom was *Emiliana huxleyi*. They presented, in a small figure, plots of reflectances at 443nm and cell counts of coccolithophores found in the English Channel surface water. This figure was enlarged and gridded to permit 23 cell-count/ml and reflectance-value data pairs to be obtained. (Note: these values were read from a graph and are therefore approximate).

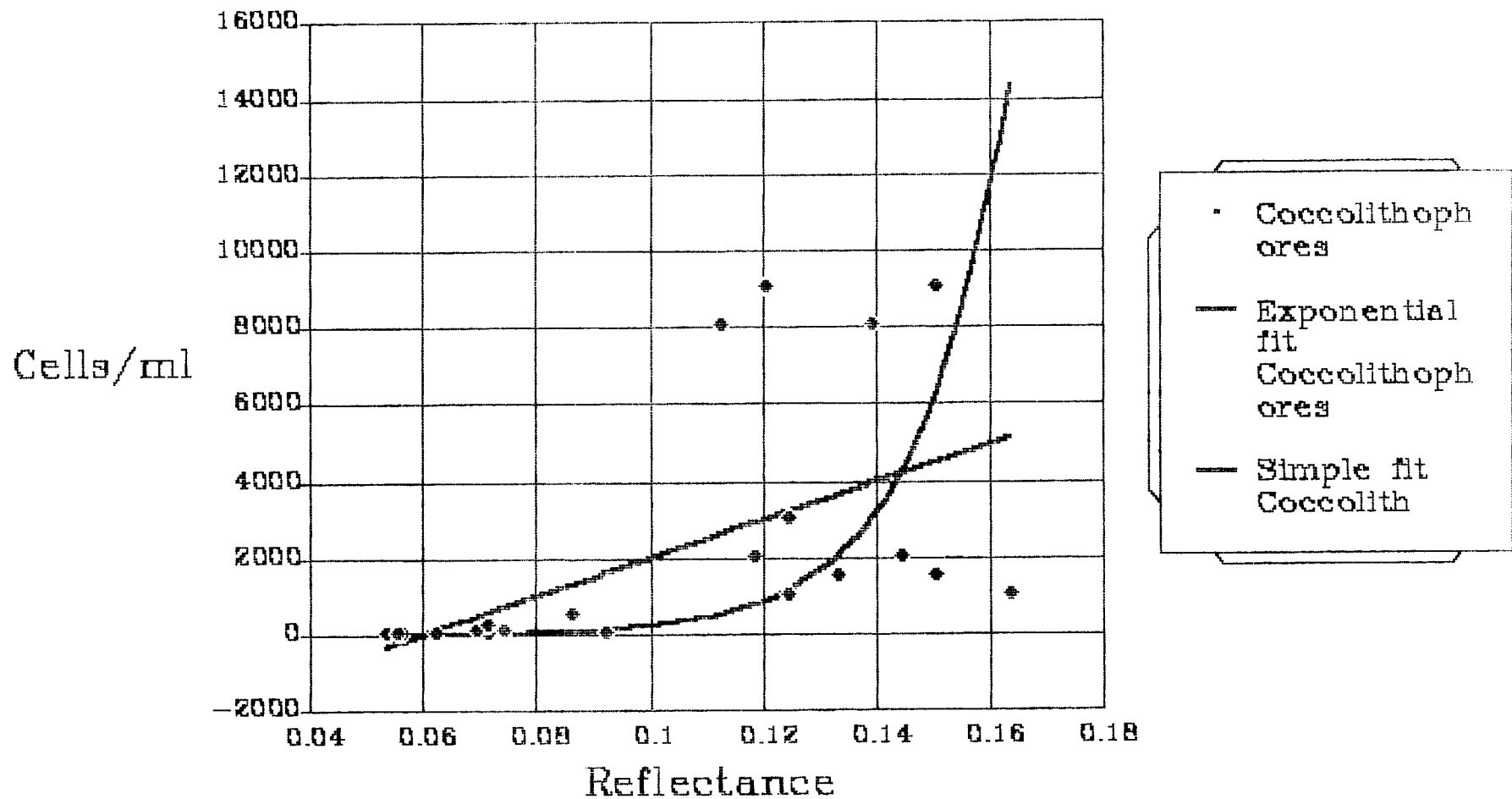
A linear regression of reflectance on cell-count/ml was calculated ($r^2 = 0.32$ and correlation coefficient = 0.56) and plotted (Figure 1). Since a linear regression did not produce reasonable appearing results, an exponential least-square regression was calculated ($r^2 = 0.72$) and plotted (Figure 2). Reflectance was the independent variable, as it would be in a MODIS application. This algorithm form is appropriate for MODIS use. Of course, pixels with "significant reflectance" (or "excess scattering") at 670nm must be identified before this algorithm may be applied.

Holligan, P. M., M. Viollier, D.S. Harbour, P. Camus, and M. Champagne-Philippe, 1983: Satellite and ship studies of coccolithophore production along a continental shelf edge. Nature, 304, 339-342.

Coccolithophores



Coccolithophores



| PRELIMINARY ESTIMATES OF MODIS CORE DATA PRODUCT ACCURACIES, AND THEIR RELEVANCE TO KEY EARTH SCIENCE ISSUES | SCIENCE QUESTION ADDRESSED | | | | | | ESTIMATED ACCURACY OF MODIS CORE DATA PRODUCT | |
|--|----------------------------|---|---|---|---|---|---|-------------|
| I. ATMOSPHERE CORE DATA PRODUCT ANALYSES | 1 | 2 | 3 | 4 | 5 | 6 | PRESENT-DAY | MODIS-ERA |
| A. <u>Total Column Ozone</u> B. <u>Aerosol Optical Depth</u> C. <u>Aerosol Size Distribution</u> D. <u>Aerosol Mass Loading</u> E. <u>Aerosol Single Scattering Albedo</u> F. <u>Lifted Index</u> G. <u>Temperature and Moisture Profiles</u> H. <u>Total Precipitable Water</u> I. <u>Cloud Fractional Area</u> J. <u>Cloud Area and Perimeter</u> K. <u>Cloud Optical Thickness</u> L. <u>Cloud Effective Emissivity</u> M. <u>Cloud Top Pressure</u> N. <u>Cloud Top Temperature</u> O. <u>Cloud Water Thermodynamic Phase</u> P. <u>Cloud Droplet Effective Radius</u> | I | | | | | I | ±10% | ±10% |
| | I | I | | | | D | ±.05 | ±.05 |
| | I | I | | | | D | ±10% | ±10% |
| | I | I | | | | D | ±40% | ±30% |
| | I | I | | | | D | ±.01 | ±.01 |
| | | | D | | | | ±3°C | ±3°C |
| | | | I | | I | | ±2°C | ±1°C |
| | | | | | D | | ±½cm | ±½cm |
| | D | | D | D | | | ±10% absol. | ±10% absol. |
| | | | D | D | | | ± | ± |
| | D | | D | D | | | ±50% absol. | ±20% absol. |
| | | | D | D | | | ±20% absol. | ±20% absol. |
| | | | D | | | | ±25 to 50mb | ±25 to 50mb |
| | | | D | | | | ±2°C | ±1°C |
| | | | D | | | | N/A | Possible |
| | | | D | | | | ±10% | ±10% |
| II. LAND CORE DATA PRODUCT ANALYSES | 1 | 2 | 3 | 4 | 5 | 6 | PRESENT-DAY | MODIS-ERA |
| A. <u>Vegetation Indices</u> B. <u>Surface Temperature</u> C. <u>Thermal Anomalies</u> D. <u>Spectral Surface Albedo</u> E. <u>Snowcover</u> F. <u>Level-2 Land-Leaving Radiances</u> G. <u>Level-1 Topographic Corrections</u> H. <u>Surface Water Cover Mapping</u> | | D | | | D | | ±0.1 | ±.04 |
| | | D | | D | D | | ±10C | ±2°C |
| | | D | | | D | | ±50°C | ±5°C |
| | | | | D | D | | ±.01 | ±.01 |
| | | | | D | | | N/A | N/A |
| | I | | | I | I | | ±20% | ±10% |
| | I | | | I | I | | ±½km | 100m |
| | | | | | D | | N/A | N/A |
| III. OCEAN CORE DATA PRODUCT ANALYSES | 1 | 2 | 3 | 4 | 5 | 6 | PRESENT-DAY | MODIS-ERA |
| A. <u>Sea Surface Temperatures</u> B. <u>Sea Ice</u> C. <u>Water Leaving Radiance</u> D. <u>Chlorophyll Fluorescence</u> E. <u>Chlorophyll-A Pigment Concentration</u> F. <u>Case-II Waters Chlorophyll-A Pigment Concentration</u> G. <u>Detached Coccolith Concentration</u> H. <u>Surface Incident Photosynthetically Active Radiation</u> I. <u>Attenuation at 490nm</u> J. <u>Attenuation of Photosynthetically Active Radiation</u> K. <u>Primary Productivity</u> . <u>Angstrom Exponent</u> M. <u>Single Scattering Aerosol Radiation</u> N. <u>In-situ Validation Observations</u> | D | | D | D | | | ±2°C | ±1°C |
| | I | | | D | | | Yes, if 25% | Yes, if 25% |
| | D | | | | | | ±10% | ±7% |
| | D | | | | | | N/A | ±50 to 100% |
| | D | | | | | | ±35% | ±20% |
| | D | | | | | | 300% | ±50% |
| | D | | | | | | N/A | ±35% |
| | D | | | | | | ±40% | ±25% |
| | D | | | | | | ±35%; R ² =0.3 | ±20% |
| | D | | | | | | N/A | ±20% |
| | D | | | | | | R ² = 0.30 | ±? |
| | I | | | | D | | ±20% | ±15% |
| | I | | | | D | | ±10% | ±6% |
| | I | | I | | | | Instr. Dep. | Instr. Dep. |

Notes: "D" indicates that a science question/issue is directly addressed.
"I" indicates that a science question/issue is indirectly addressed.

Total Column Ozone

Susskind, J., J. Rosenfield, D. Reuter, and M. T. Chahine, 1984: Remote sensing of weather and climate parameters from HIRS2/MSU on Tiros-N, J. Geophys. Res., 89D, 4677-4697.

Aerosol Optical Depth

News and Notes, 1989: AVHRR derived aerosol optical thickness products archived, Bull. Amer. Meteor. Soc., 70, 1155.

Tanre, D., P. Y. Deschamps, C. Devaux, and M. Herman, 1988: Estimation of saharan aerosol optical thickness from blurring effects in thematic mapper data, J. Geophys. Res., 93D, 15955-15964.

Aerosol Size Distribution

Spinhirne, J. D., and M. D. King, 1985: J. Geophys. Res., 90C, 10,607.

Aerosol Mass Loading

Fraser, R. S., Y. J. Kaufman, and R. L. Mahoney, 1984: Satellite measurements of aerosol mass and transport, Atmos. Environ., 18, 2577-2584.

Aerosol Single Scattering Albedo

Kaufman, Y. J., 1987: Satellite sensing of aerosol absorption, J. Geophys. Res., 92D, 4307-4317.

Lifted Index

Bolton, D., 1980: The computation of equivalent potential temperature, Mon. Wea. Rev., 108, 1046-1053.

Temperature and Moisture Profiles

Menzel, P., 1983: An evaluation of atmospheric soundings from geostationary satellites, Appl. Optics, 22, 2686.

Menzel, P., 1981: First sounding results from VAS-D, Bull. Amer. Meteor. Soc., 20, 3641.

Reuter, D., J. Susskind, and A. Pursh, 1988: First guess dependence of a physically based set of temperature-humidity retrievals from HIRS2/MSU data, J. Atm. Ocean. Tech., 5, 70-83.

Susskind, J., J. Rosenfield, and D. Reuter, 1983: An accurate radiative transfer model for use in the direct physical inversion of HIRS2 and MSU temperature sounding data, J. Geophys. Res., 88C, 8550-8568.

Total Precipitable Water

Reuter, D., J. Susskind, and A. Pursh, 1988: First guess dependence of a physically based set of temperature-humidity retrievals from HIRS2/MSU data. J. Atm. Ocean. Tech., 5, 70-83.

Cloud Fractional Area

The error should be 0.10. The determination becomes less accurate as the fractional coverage decreases.

Wielicki, B. A. and J. A. Coakley, Jr., 1981: Cloud retrieval using infrared sounder data: error analysis, J. Appl. Meteor., 20, 157.

Susskind, J., D. Reuter, and M. T. Chahine, 1987: Cloud fields derived from analysis of HIRS2/MSU sounding data, J. Geophys. Res., 92D, 4035-4050.

Cloud Area and Perimeter

Cloud Optical Thickness

This algorithm is expected to achieve accuracies of 3% for very thick uniform clouds. A more reasonable error estimate may be 0.2 in the optical depth estimate.

King, M. D., 1987: Determination of the scaled optical thickness of clouds from reflected solar radiation measurements, J. Atmos. Sci., 44, 1734.

Nakajima, T., and M. D. King, 1989: Determination of the optical thickness and effective particle radius of clouds from reflected solar radiation measurements. Part I: Theory, J. Atmos. Sci., in press.

Cloud Effective Emissivity

The error should be estimated as 0.20. The actual error will be a function of the measured value. The determination will be more accurate for larger values, i.e., the absolute error will be larger for small effective emissivity than for large effective emissivity.

Eyre, J. R., and W. P. Menzel, 1989: Retrieval of cloud parameters from satellite sounder data: a simulation study, J. Appl. Meteor., 28, 267.

Cloud Top Pressure

The error should be ± 50 mb. The accuracy increases for thicker clouds.

Wylie, D. P. and W. P. Menzel, 1989: Two years of cloud cover statistics using VAS, J. Climate, 2, 380.

Cloud Top Temperature

For sufficiently thick clouds, the temperature uncertainty is equivalent to the uncertainty in the thermal infrared brightness temperature. The uncertainties in pressure determination and profiles will determine the error for thinner clouds.

Wielicki, B. A. and J. A. Coakley, Jr., 1981: Cloud retrieval using infrared sounder data: error analysis, J. Appl. Meteor., 20, 157.

Cloud Water Thermodynamic Phase

Cloud Droplet Effective Radius

Nakajima, T., and M. D. King, 1989: Determination of the optical thickness and effective particle radius of clouds from reflected solar radiation measurements. Part I: Theory, J. Atmos. Sci., in press.

Vegetation indices

Estimated accuracy of NDVI is ± 0.1 presently, and ± 0.04 in the future for canopies such that the NDVI is greater than 0.2. When the NDVI is less than 0.2, the accuracy deteriorates. Specific accuracy estimates are not contained in the PIs' proposals. Reasonableness of the estimates are based on personal communications with Garrick Gutmann (NOAA/NESDIS) and Sam Goward (U of MD).

Estimated accuracy of SAVI is ± 0.025 at present.

Huete, A. R., 1988: A Soil-Adjusted Vegetation Index (SAVI), Remote Sensing of the Environment, 25, 295-309.

Surface temperature

Wan, Zhengming, Land Surface Temperature Measurements from Eos MODIS Data, Proposal Submitted to NASA, June 1988.

Thermal anomalies

Thermal Anomalies ± 50 °C at present, and ± 5 °C in the MODIS era.

Fires and other high temperature events very reliably detected--supporting references:

Kaufman, Yoram J., Global Monitoring of Aerosols Properties - Aerosol Climatology, Atmospheric Corrections, Biomass Burning, and Aerosol Effect on Clouds and Radiation, MODIS Team Member Proposal, June, 1988

Stephens, George, and Michael Matson, Regional and Global Fire Detection Using AVHRR Data, Presentation at the Twenty-First International Symposium on Remote Sensing of the Environment, Ann Arbor, Michigan, October 26-30, 1987.

Temperature accuracies are estimates for whole pixel scenes based on presently existing instruments and required MODIS capabilities and expected global surface temperature accuracy for normal, non-anomalous land surfaces.

Preliminary Specification for the Moderate-Resolution Imaging Spectrometer - Nadir (NADIR), GSFC-415-EOS-00006, Goddard Space Flight Center, Greenbelt, MD 21044, September 18, 1989

Spectral surface albedo

Kaufman, Y. J. and C. Sendra, 1988: Algorithm for automatic corrections to visible and near-IR satellite imagery, Int. J. Remote Sensing, 9, 1357-1381.

Kaufman, Y. J., 1988: Atmospheric effect on spectral signature - measurements and corrections, IEEE Trans. Geosciences and Remote Sensing, 26, 441-450.

Snowcover

Rossow, W. B., C. L. Brest, and L. C. Garder Global, 1989: Seasonal surface variations from satellite radiance measurements, J. Climate, 2, 214-247.

Rossow, W. B., L. C. Garder, and A. A. Lacis Global, 1989: Seasonal cloud variations from satellite radiance measurements, Part 1: sensitivity of analysis, J. Climate, 2, 419-458.

Level 2-Land Leaving Radiances

Level-1 Topographic Corrections

Surface Water-Cover Mapping

Sea Surface Temperatures

McClain, E. P., W. G. Pichel, and C. C. Walton, 1985: Comparative performance of AVHRR-based multichannel sea surface temperatures, J. Geophys. Res., 90, 11,587-11,601.

AVHRR ± 0.3 °C:

G. Ohring et.al., Trans. Amer. Geophys. U., 70, October 10, 1989.

Sea Ice

Can unambiguously determine the presence of sea-ice if the pixel is at least 25% sea-ice covered.

Rossow, W. B., L. C. Garder, and A. A. Lacis, 1989: Global, seasonal cloud variations from satellite radiance measurements, Part 1: sensitivity of analysis. J. Climate, 2, 419-458.

Water Leaving Radiance

Gordon, H. R., D. K. Clark, J. W. Brown, O. B. Brown, R. H. Evans, and W. W. Broenkow, 1983: Phytoplankton pigment concentrations in the Middle Atlantic Bight: comparison of ship determinations and CZCS estimates, Applied Optics, 22, 20-36.

Chlorophyll Fluorescence

The accuracies are about $\pm 100\%$ when chlorophyll-a concentrations are low, and about $\pm 50\%$ when chlorophyll-a concentrations are high.

Gower, J. F. R. and G. A. Borstad, 1987: On the use of the solar-stimulated fluorescence signal from chlorophyll a for airborne and satellite mapping of phytoplankton, Advances in Space Research, 7, 101-106.

Chlorophyll-A Pigment Concentration

Gordon, H. R., D. K. Clark, J. W. Brown, O. B. Brown, R. H. Evans, and W. W. Broenkow, 1983: Phytoplankton pigment concentrations in the Middle Atlantic Bight: comparison of ship determinations and CZCS estimates, Applied Optics, 22, 20-36.

Assuming improvement due to the validation program of D.K. Clark.

Case-II Waters Chlorophyll-A Pigment Concentration

Carder, K. L. 1989: High spectral resolution MODIS-T algorithms for ocean chlorophyll in Case II waters, Eos Team Member Proposal.

Detached Coccolith Concentration

The accuracy is ± 2700 cells/ml (out of a maximum observed value of 9000 cells/ml) when reflectances are the independent variable using a linear regression. The accuracy is ± 0.03 (in fractional reflectance) when cells per milliliter are the independent variable. For the algorithm to work, the presence of coccoliths must first be identified through the diagnosis of "excess scattering."

Holligan, P. M., M. Viollier, D. S. Harbour, P. Camus, and M. Champagne-Philippe, 1983: Satellite and ship studies of coccolithophore production along a continental shelf edge, Nature, 304, 339-342.

Surface Incident Photosynthetically Active Radiation

Present errors are 21 Wm_{-2} RMS at local noon for both clear and cloudy conditions.

Kuring, N., M. R. Lewis, T. Platt, and J. E. O'Reilly, 1989: Satellite-derived estimates of primary productivity on the northwest Atlantic continental shelf, Continental Shelf Research, 89, in press.

Expected MODIS-era errors are 13 Wm_{-2} RMS at local noon for both clear and cloudy conditions, based on the expectation that MODIS algorithms will perform as well as GOES, using the Gautier and Katsaros model.

Gautier, C. and K. B. Katsaros, 1989: Insolation during STREX: Part I, comparisons between surface measurements and satellite estimates, J. Geophys. Res., 89, 11,779-11,788.

Attenuation at 490nm

$R^2=0.91$ (based on dependent data)

Austin, R. W. and T. J. Petzold, 1983: The determination of the diffuse attenuation coefficient of sea water using the Coastal Zone Color Scanner, In Oceanography from Space, J.F.R. Gower, ed., 239-256.

This algorithm is based on the determination of chlorophyll, so its accuracy is dependent upon the chlorophyll retrieval accuracy, which is expected to improve with MODIS.

Gordon, H. R., D. K. Clark, J. W. Brown, O. B. Brown, R. H. Evans, and W. W. Broenkow, 1983: Phytoplankton pigment concentrations in the Middle Atlantic Bight: comparison of ship determinations and CZCS estimates, Applied Optics, 22, 20-36.

Attenuation of Photosynthetically Active Radiances

This algorithm is based on the determination of chlorophyll, so its accuracy is dependent upon the chlorophyll retrieval accuracy.

Primary Productivity

Balch, W. M., M. R. Abbott, and R. W. Eppley, 1989: Remote sensing of primary production--I, A comparison of empirical and semi-analytical algorithms, Deep-Sea Research, 36, 281-295.

Angstrom Exponent

Single Scattering Aerosol Radiances

Gordon, H. R., D. K. Clark, J. W. Brown, O. B. Brown, R. H. Evans, and W. W. Broenkow, 1983: Phytoplankton pigment concentrations in the Middle Atlantic Bight: comparison of ship determinations and CZCS estimates, Applied Optics, 22, 20-36.

Gordon, H. R. and D. J. Castano, 1989: Aerosol analysis with the coastal zone color scanner: a simple method for including multiple scattering effects, Applied Optics, 28, 1320-1326.

In-situ Validation Observations

The in-situ observations are derived from moored and drifting buoys, and include physical, biological, and optical instruments and measurements.

Clark, D. K., 1988: Marine Optical Characterization, Proposal for NASA in response to AO# OSSA-1-88.